SURFACE EROSION UNDER CLUSTER ION IMPLANTATION: CRATER AND HILLOCK FORMATION

V.N. Popok, S.V. Prasalovich and E.E.B. Campbell
Goteborg University & Chalmers University of Technology, Goteborg, 41296, Sweden
fax: +46-31-7723496, e-mail: popok@fy.chalmers.se

Silicon samples implanted by small mass-selected Ar_n^+ and $(N_2)_n^+$ cluster ions with energies in the range of 3-18 keV/cluster are studied using atomic force microscopy. Control samples implanted by Ar^+ ions with the energies of 1.5-6.0 keV are used for comparison. The images show surface erosion appearing as simple and complex crater formation in the cases of both monomer and cluster bombardment. The complex craters with centre-positioned cone-shaped hillocks are surrounded by low-height rims (~0.5 nm). The hillock height varies on a few nm scale depending on the implantation energy, cluster size and species. A simple model explaining the hillock formation with relation to the thermal-transfer effect at the collision spot is proposed.

Introduction

Ion beam technologies have attained an advanced stage of development. However, nowadays fabrication of nanometre-scale structures needs much more controllable and versatile tools on an atomistic scale. In the last decade there has been a growing interest in using cluster ion beams as an alternative to beams of monomer ions [1]. Since the middle of the 90's a number of research groups have been involved in the study of cluster ion beams.

Specific phenomena at cluster-surface impact allow one to divide the use of clusters into two conditional cases: low-energy and high-energy regimes. There is no precise dividing line on the energy scale for those two cases. However, one can consider a process as low-energy when the energy per atom of the accelerated cluster is below or the same as the binding energy of constituents in the cluster. It is so-called soft landing of clusters. In this paper we mainly discuss the other regime, i.e. when the energy of a cluster constituent atom is over both the constituents binding energy (the cluster breaks down under the energetic impact) and the penetration threshold energy of a target material.

Due to the large size and weak bonding of atoms the cluster-surface impact is fundamentally different from that of monomers [2]. The cluster size usually exceeds a target unit cell size. Hence, nuclear stopping (direct collisions with target atoms) dominates for clusters from the first atomic layer of the substrate. Clusters generate multiple-collision effects with lower energies. An acceleration of, for example, 100 atoms cluster to 10 keV provides 100 eV energy to each constituent atom. However, multiplication of this relatively low energy by the number of atoms and dividing by very small surface collision area leads to high density of energy deposited by the cluster.

It is generally recognised that the cluster-solid interaction is non-linear which gradually increases with cluster size. The nonlinearity arises from the fact that the cluster atoms influence each other during the penetration into the target. Since the cluster breaks down into single atoms quite rapidly under impact, one can expect an overlapping of the collision cascades originating from individual cluster atoms. Thus, the difference between the stopping of an atom in a cluster and a single atom can make some difference in the projected range of cluster constituents and produced radiation damage compared to monomer ion implantation. Molecular dynamic (MD) and Monte Carlo simulations show that the penetration depth of clusters is larger than for the corresponding ions at the same incident velocity [3]. It was suggested that a so-called clearing-the-way effect, where the "front" atoms of the cluster push target atoms out of the way, could take place. Recent MD simulations, confirmed by experiments on Au_7, Ag_7 and Si_7 cluster implantation into graphite, report a linear dependence of the implantation range with the momentum of the clusters [4].

Energetic impact of a large cluster creates a violent interaction between atoms in the central zone where equivalent temperature and pressure may reach 10^5 K and 10^6 bar, respectively [5], leading to a number of additional effects: thermal spike, shock wave, elastic rebound etc. By both MD simulations and experiments it was shown that cluster impact could cause surface erosion or crater formation [5-7]. Along with craters, hillocks (nm-size protrusions) are found [5, 8-10]. For low-energy cluster implantation (tens keV), surface erosion effects are only beginning to be studied experimentally and present great interest to provide successful material modification using cluster implantation.

Experimental

An assembly called PUCLUS (PUlsed CLUster Source) allowing cluster production from gaseous precursors and subsequent cluster ion beam acceleration, focussing and steering was used [10]. Si samples were bombarded by size-selected $(N_2)_n^+$ and Ar_n^+ cluster ions (n from 12 to 55) with energies of 3-18 keV at normal impact angle to the surface. Control samples were implanted by Ar^+ ions with energies of 1.5-6.0 keV. The fluences in all cases were low (10^8-10^{10} cm^{-2}) and this can be considered as single impact conditions. Implantation was performed in residual vacuum of $(1\text{-}2)\times10^{-6}$ mbar. Images of the surfaces after cluster and monomer collisions were obtained using atomic force microscopy (AFM) in the tapping mode.

Results and discussion

Bombardment by 1.5 keV Ar^+ monomer ions leads to crater and hillock formation on the surface as shown in Fig. 1. The hillocks are found to be located in the centre of the craters. These structures are called complex craters by analogy with those formed by meteorite impact on a planet surface and have the same complexity. The appearance of simple craters and hillocks in the case of ion-surface impact is a known phenomenon [11, 12]. Craters are

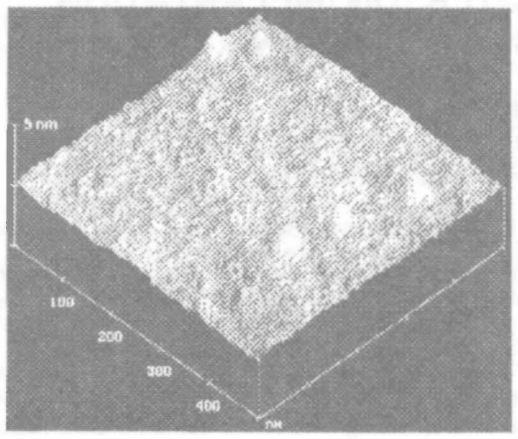

Fig. 1. AFM image of Si surface implanted by 1.5 keV Ar^+ ions

formed as a result of local excavation of the target material (sputtering) on impact. The hillock formation was explained by a thermal spike effect. The spike is initiated by energy deposited in ion-atom and atom-atom impact during the ballistic phase of the collision cascade in the target.

However, complex craters consisting of central cone-shaped hillock and surrounding rim are observed here for the first time. The simple crater diameter and hillock basal diameter is of the same value, about 10-15 nm. Wall to wall diameter of the rims in the complex craters is about 20-40 nm. Unfortunately, the observed lateral dimensions of the hillocks are probably enlarged and the shape is slightly distorted because of their convolution with the shape and curvature radius (about 10 nm) of the AFM tips used. However, the height of the hillocks is estimated with high precision, it varies from 0.5 to 1.5 nm. The increase of implantation energy leads to the hillocks gradual disappearance, their height becomes comparable with the rim height (ca. 0.5 nm). At an energy of 6 keV hillocks are not found.

In the case of Ar_{12}^+ cluster ion bombardment simple and complex craters similar to those found for the control samples are observed. Complex craters (with hillocks) are prevailing on the AFM images. The mean crater diameter is not changed significantly compared to the control samples. However, the hillocks are found to be higher, from 1.5 to 3.0 nm for the implantation energies of 3-9 keV. Unfortunately, any systematic dependence of the hillock height on the energy for this range is not found. With further implantation energy increase the hillocks start gradually disappearing within the craters, their height becomes comparable with the rim height (Fig. 2a). Complex craters in this case are very similar to those formed by meteorite impact (Fig. 2b). Implantation of Ar_{22} cluster ions shows the same tendency in complex crater formation and hillock height decrease with energy. However the maximal hillock height does not exceed 1.5 nm for this cluster size. The simple craters and complex craters with hillocks just slightly towered inside are preferably formed by the implantation of larger clusters Ar_{32} and Ar_{55} (Fig. 3).

Nitrogen cluster ion implantation also leads to complex crater formation on the Si surface. Crater and hillock diameters are comparable with those above-reported. But, at the same implantation energy and close cluster mass (in a.m.u.), the hillocks are higher (up to 5 nm) after the nitrogen cluster ion implantation compared to the case of argon.

Modelling for a 2-layered target consisting of 2 nm thick native SiO_2 and bulk Si using TRIM-2003 [13] gives us the ion projected range of $R_p \approx 4.7 \pm 1.8$ nm for 1.5 keV Ar^+ ions. The simulation shows that about 70 % and 25 % of total ion energy are lost on phonon formation and ionisation, respectively. Those two effects lead to effective heat transfer to the matrix. Although the ions stop in the bulk Si, the maxima of energy lose on the phonon formation and ionisation are located in the surface SiO_2 layer and at the SiO_2/Si boundary. In the case of cluster implantation, the SRIM simulated data corresponds only approximately to the real processes due to multi-collisional and other non-linear effects. However, the result of simulation on efficient phonon formation and ionisation explains a considerable heat-transfer effect. MD simulations of cluster-surface impact for various species and target materials also show that the local temperatures in the collision area can significantly exceed the melting point of the target material [5, 14, 15].

Hence, one can assume that the hillocks are a result of a local thermal effect causing shallow-layer melting at the collision spot with subsequent liquid melt out and quenching. The shock wave phenomenon can also play an important role in the hillock and crater formation especially for impact of large clusters. The hillock disappearance with the implantation energy increase can be explained by an inward shift

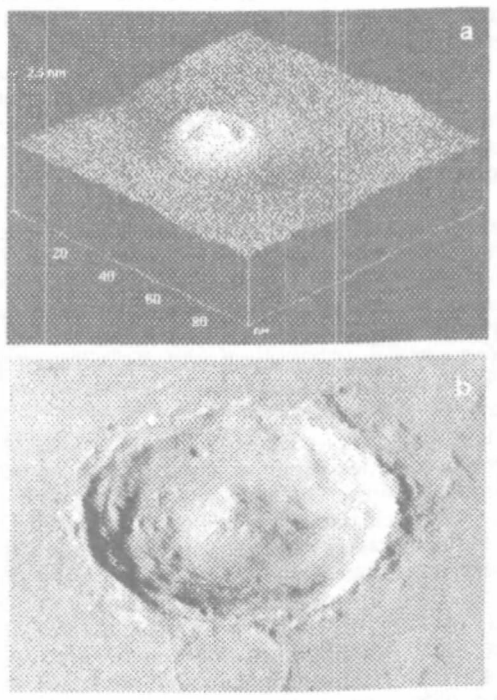

Fig. 2. AFM image of complex crater with diameter of 18 nm on Si surface implanted by 18 keV Ar_{12} clusters (a) and Yuti crater on Mars with diameter of 18 km as imaged by Viking Orbiter (b) [16]

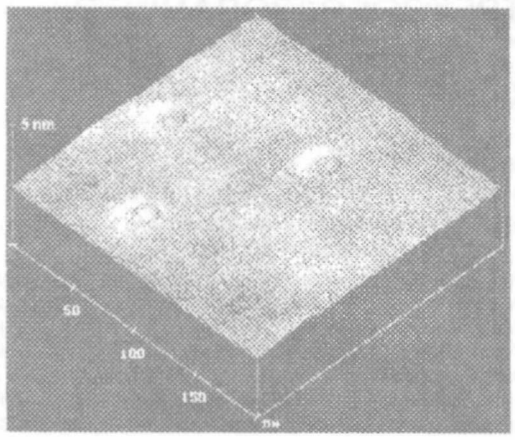

Fig. 3. AFM image of Si surface implanted by 15 keV Ar_{55}^+ cluster ions

of the "phonon and ionisation maxima" eliminating the melting and "pushing away" effects in the surface layer. In the case of large Ar clusters compared to the smaller ones implanted with the same energy, the cluster energy dissipates in a larger volume decreasing the melting effect. That is why the hillocks are just slightly pronounced in the craters (see Fig. 3). The observed difference in the hillock height for the argon and nitrogen cluster implantation allow us to suggest a difference in the cluster-to-target energy-transfer processes, i.e. in stopping of the cluster constituents, for the various cluster species.

Conclusion

Results on impact of cluster and monomer ions with silicon surfaces are studied using the AFM technique. Formation of complex craters consisting of a centre-positioned hillock and surrounding rim is observed in the both cases. Crater and hillock parameters are studied depending on cluster species, size and implantation energy. The hillock formation is explained by a kinetic energy transfer from the ion or cluster constituents to the target causing shallow-layer melting at the collision spot with subsequent liquid melt out and quenching. A simple phenomenological model taking into account intensive phonon formation and ionisation processes in the surface layer under monomer and cluster ion bombardment is suggested to explain the possible channels for energy transfer and local target heating.

Authors acknowledge support from the Goran Gustafsson Foundation for Research in Natural Science and Medicine and The Swedish Research Council (grant No. 621-2002-5387).

References

1. *Milani P., Iannotta S.* Cluster Beam Synhtesis of Nanostructured Materials. – Berlin, Heidelberg: Springer-Verlag, 1999. – 190 p.
2. *Takagi T.* // Mat. Sci. Eng. – 1998. – V. A253. – P. 30.
3. *Meiwes-Broer K.-H.* Metal Clusters at Surfaces. – Berlin: Springer, 2000. – 145 p. and references there.
4. *Pratontep S., Preece P., Xirouchaki C. et al.* // Phys. Rev. Let. – 2003. – V. 90, No 5. – P. 055503-1.
5. *Allen L.P., Insepov Z., Fenner D.B. et al.* // J. Appl. Phys. – 2002. – V. 92, No 7. – P. 3671.
6. *Averback R.S., De la Rubia T., Hsieh H., Benedek R.* // Nucl. Instrum. Meth. B – 1991. – V. 59/60. – P. 709.
7. *Yamaguchi Y., Gspann J.* // Phys. Rev. B. – 2002. – V. 66. – P. 155408.
8. *Gruber A., Gspann J.* // J. Vac. Sci. Technol. B – 1997. – V. 15. – P. 2362.
9. *Song J.-H., Kwon S.N., Choi D.-K., Choi W.-K.* // Nucl. Instr. Meth. B. – 2001. – V. 179. – P. 568.
10. *Popok V.N., Prasalovich V.S., Campbell E.E.B.* // Nucl. Instrum. Meth. B. – 2003. – V. 207, No 2. – P. 145.
11. *Merkle K.L., Jager W.* // Phil. Mag. A – 1981. – V. 44. – P. 741.
12. *Yang Q., Li T., King B., MacDonald R.J.* // Phys. Rev. B – 1996. – V. 53. – P. 3032.
13. *Ziegler J.F.* The stopping and range of ions in matter (SRIM-2003). <www.SRIM.org>.
14. *Colla T.J., Aderjan R., Kissel R., Urbassek M.* // Phys. Rev. B. – 2000. – V. 62, No. 12. – P. 8487.
15. *Yamaguchi Y., Gspann J.* // Phys. Rev. B. – 2002. – V. 66. – P. 155408.
16. Picture downloaded from <www.lpi.usra.edu>.